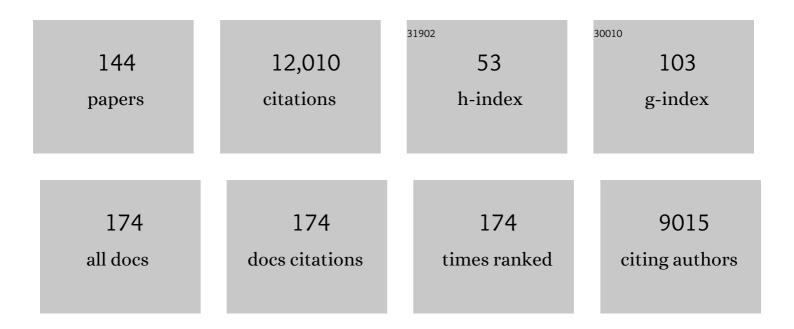
List of Publications by Year in descending order

Source: https://exaly.com/author-pdf/3574218/publications.pdf Version: 2024-02-01



#	Article	IF	CITATIONS
1	Particulate emissions of real-world light-duty gasoline vehicle fleet in Iran. Environmental Pollution, 2022, 292, 118303.	3.7	5
2	Source identification and characterization of organic nitrogen in atmospheric aerosols at a suburban site in China. Science of the Total Environment, 2022, 818, 151800.	3.9	3
3	Modelling the gas–particle partitioning and water uptake of isoprene-derived secondary organic aerosol at high and low relative humidity. Atmospheric Chemistry and Physics, 2022, 22, 215-244.	1.9	8
4	Survival of newly formed particles in haze conditions. Environmental Science Atmospheres, 2022, 2, 491-499.	0.9	8
5	Elucidating the present-day chemical composition, seasonality and source regions of climate-relevant aerosols across the Arctic land surface. Environmental Research Letters, 2022, 17, 034032.	2.2	9
6	Equal abundance of summertime natural and wintertime anthropogenic Arctic organic aerosols. Nature Geoscience, 2022, 15, 196-202.	5.4	31
7	Organic aerosol source apportionment by using rolling positive matrix factorization: Application to a Mediterranean coastal city. Atmospheric Environment: X, 2022, 14, 100176.	0.8	4
8	Fragment ion–functional group relationships in organic aerosols using aerosol mass spectrometry and mid-infrared spectroscopy. Atmospheric Measurement Techniques, 2022, 15, 2857-2874.	1.2	3
9	Synergistic HNO3–H2SO4–NH3 upper tropospheric particle formation. Nature, 2022, 605, 483-489.	13.7	26
10	European aerosol phenomenology â^' 8: Harmonised source apportionment of organic aerosol using 22 Year-long ACSM/AMS datasets. Environment International, 2022, 166, 107325.	4.8	41
11	High-frequency gaseous and particulate chemical characterization using extractive electrospray ionization mass spectrometry (Dual-Phase-EESI-TOF). Atmospheric Measurement Techniques, 2022, 15, 3747-3760.	1.2	7
12	Online detection of trace volatile organic sulfur compounds in a complex biogas mixture with proton-transfer-reaction mass spectrometry. Renewable Energy, 2022, 196, 1197-1203.	4.3	2
13	Determination of the collision rate coefficient between charged iodic acid clusters and iodic acid using the appearance time method. Aerosol Science and Technology, 2021, 55, 231-242.	1.5	18
14	Comparison of five methodologies to apportion organic aerosol sources during a PM pollution event. Science of the Total Environment, 2021, 757, 143168.	3.9	19
15	Molecular characterization of ultrafine particles using extractive electrospray time-of-flight mass spectrometry. Environmental Science Atmospheres, 2021, 1, 434-448.	0.9	10
16	Role of iodine oxoacids in atmospheric aerosol nucleation. Science, 2021, 371, 589-595.	6.0	94
17	A new method for long-term source apportionment with time-dependent factor profiles and uncertainty assessment using SoFi Pro: application to 1 year of organic aerosol data. Atmospheric Measurement Techniques, 2021, 14, 923-943.	1.2	50
18	Influence of biomass burning vapor wall loss correction on modeling organic aerosols in Europe by CAMx v6.50. Geoscientific Model Development, 2021, 14, 1681-1697.	1.3	5

#	Article	IF	CITATIONS
19	Large contribution to secondary organic aerosol from isoprene cloud chemistry. Science Advances, 2021, 7, .	4.7	24
20	Brown Carbon in Primary and Aged Coal Combustion Emission. Environmental Science & Technology, 2021, 55, 5701-5710.	4.6	31
21	Photodegradation of α-Pinene Secondary Organic Aerosol Dominated by Moderately Oxidized Molecules. Environmental Science & Technology, 2021, 55, 6936-6943.	4.6	11
22	Characterization of primary and aged wood burning and coal combustion organic aerosols in an environmental chamber and its implications for atmospheric aerosols. Atmospheric Chemistry and Physics, 2021, 21, 10273-10293.	1.9	17
23	Source-specific light absorption by carbonaceous components in the complex aerosol matrix from yearly filter-based measurements. Atmospheric Chemistry and Physics, 2021, 21, 12809-12833.	1.9	15
24	Effects of aerosol size and coating thickness on the molecular detection using extractive electrospray ionization. Atmospheric Measurement Techniques, 2021, 14, 5913-5923.	1.2	7
25	The driving factors of new particle formation and growth in the polluted boundary layer. Atmospheric Chemistry and Physics, 2021, 21, 14275-14291.	1.9	38
26	Modeling the effect of reduced traffic due to COVID-19 measures on air quality using a chemical transport model: impacts on the Po Valley and the Swiss Plateau regions. Environmental Science Atmospheres, 2021, 1, 228-240.	0.9	12
27	Structures and reactivity of peroxy radicals and dimeric products revealed by online tandem mass spectrometry. Nature Communications, 2021, 12, 300.	5.8	28
28	Highly time-resolved measurements of element concentrations in PM ₁₀ and PM _{2.5} : comparison of Delhi, Beijing, London, and Krakow. Atmospheric Chemistry and Physics, 2021, 21, 717-730.	1.9	19
29	Online monitoring of volatile organic compounds emitted from human bronchial epithelial cells as markers for oxidative stress. Journal of Breath Research, 2021, 15, 016015.	1.5	2
30	Photolytically induced changes in composition and volatility of biogenic secondary organic aerosol from nitrate radical oxidation during night-to-day transition. Atmospheric Chemistry and Physics, 2021, 21, 14907-14925.	1.9	14
31	Time-dependent source apportionment of submicron organic aerosol for a rural site in an alpine valley using a rolling positive matrix factorisation (PMF) window. Atmospheric Chemistry and Physics, 2021, 21, 15081-15101.	1.9	22
32	Constraining the response factors of an extractive electrospray ionization mass spectrometer for near-molecular aerosol speciation. Atmospheric Measurement Techniques, 2021, 14, 6955-6972.	1.2	10
33	Chemical composition of nanoparticles from <i>α</i> -pinene nucleation and the influence of isoprene and relative humidity at low temperature. Atmospheric Chemistry and Physics, 2021, 21, 17099-17114.	1.9	12
34	Evaluation of receptor and chemical transport models for PM10 source apportionment. Atmospheric Environment: X, 2020, 5, 100053.	0.8	41
35	Source apportionment of fine particulate matter in a Middle Eastern Metropolis, Tehran-Iran, using PMF with organic and inorganic markers. Science of the Total Environment, 2020, 705, 135330.	3.9	30
36	Sources of particulate-matter air pollution and its oxidative potential in Europe. Nature, 2020, 587, 414-419.	13.7	352

#	Article	IF	CITATIONS
37	Rapid growth of new atmospheric particles by nitric acid and ammonia condensation. Nature, 2020, 581, 184-189.	13.7	169
38	Photo-oxidation of Aromatic Hydrocarbons Produces Low-Volatility Organic Compounds. Environmental Science & Technology, 2020, 54, 7911-7921.	4.6	66
39	Online Aerosol Chemical Characterization by Extractive Electrospray Ionization–Ultrahigh-Resolution Mass Spectrometry (EESI-Orbitrap). Environmental Science & Technology, 2020, 54, 3871-3880.	4.6	25
40	Enhanced growth rate of atmospheric particles from sulfuric acid. Atmospheric Chemistry and Physics, 2020, 20, 7359-7372.	1.9	58
41	Real-time measurement and source apportionment of elements in Delhi's atmosphere. Science of the Total Environment, 2020, 742, 140332.	3.9	78
42	On the fate of oxygenated organic molecules in atmospheric aerosol particles. Science Advances, 2020, 6, eaax8922.	4.7	63
43	Oxidative stress-induced inflammation in susceptible airways by anthropogenic aerosol. PLoS ONE, 2020, 15, e0233425.	1.1	19
44	Molecular understanding of the suppression of new-particle formation by isoprene. Atmospheric Chemistry and Physics, 2020, 20, 11809-11821.	1.9	49
45	Overview: Integrative and Comprehensive Understanding on Polar Environments (iCUPE) – concept and initial results. Atmospheric Chemistry and Physics, 2020, 20, 8551-8592.	1.9	26
46	Molecular understanding of new-particle formation from <i>α</i> -pinene between â^'50 and +25 °C. Atmospheric Chemistry and Physics, 2020, 20, 9183-9207.	1.9	68
47	Development of a versatile source apportionment analysis based on positive matrix factorization: a case study of the seasonal variation of organic aerosol sources in Estonia. Atmospheric Chemistry and Physics, 2019, 19, 7279-7295.	1.9	19
48	Infrared-absorbing carbonaceous tar can dominate light absorption by marine-engine exhaust. Npj Climate and Atmospheric Science, 2019, 2, .	2.6	71
49	A Comprehensive Nontarget Analysis for the Molecular Reconstruction of Organic Aerosol Composition from Glacier Ice Cores. Environmental Science & Technology, 2019, 53, 12565-12575.	4.6	10
50	Quantification of the impact of cooking processes on indoor concentrations of volatile organic species and primary and secondary organic aerosols. Indoor Air, 2019, 29, 926-942.	2.0	28
51	Determination of n-alkanes, polycyclic aromatic hydrocarbons and hopanes in atmospheric aerosol: evaluation and comparison of thermal desorption GC-MS and solvent extraction GC-MS approaches. Atmospheric Measurement Techniques, 2019, 12, 4779-4789.	1.2	15
52	Molecular Composition and Volatility of Nucleated Particles from α-Pinene Oxidation between â~'50 °C and +25 °C. Environmental Science & Technology, 2019, 53, 12357-12365.	4.6	32
53	Impact of anthropogenic and biogenic sources on the seasonal variation in the molecular composition of urban organic aerosols: a field and laboratory study using ultra-high-resolution mass spectrometry. Atmospheric Chemistry and Physics, 2019, 19, 5973-5991.	1.9	40
54	Effects of two different biogenic emission models on modelled ozone and aerosol concentrations in Europe. Atmospheric Chemistry and Physics, 2019, 19, 3747-3768.	1.9	36

#	Article	IF	CITATIONS
55	Primary emissions versus secondary formation of fine particulate matter in the most polluted city (Shijiazhuang) in North China. Atmospheric Chemistry and Physics, 2019, 19, 2283-2298.	1.9	74
56	Wintertime secondary organic aerosol formation in Beijing–Tianjin–Hebei (BTH): contributions of HONO sources and heterogeneous reactions. Atmospheric Chemistry and Physics, 2019, 19, 2343-2359.	1.9	83
57	Predominance of secondary organic aerosol to particle-bound reactive oxygen species activity in fine ambient aerosol. Atmospheric Chemistry and Physics, 2019, 19, 14703-14720.	1.9	31
58	Sources of organic aerosols in Europe: a modeling study using CAMx with modified volatility basis set scheme. Atmospheric Chemistry and Physics, 2019, 19, 15247-15270.	1.9	35
59	Secondary organic aerosol formation from smoldering and flaming combustion of biomass: a box model parametrization based on volatility basis set. Atmospheric Chemistry and Physics, 2019, 19, 11461-11484.	1.9	24
60	Effect of Stove Technology and Combustion Conditions on Gas and Particulate Emissions from Residential Biomass Combustion. Environmental Science & Technology, 2019, 53, 2209-2219.	4.6	35
61	Trace Metals in Soot and PM _{2.5} from Heavy-Fuel-Oil Combustion in a Marine Engine. Environmental Science & Technology, 2018, 52, 6714-6722.	4.6	112
62	Characterization of Gas-Phase Organics Using Proton Transfer Reaction Time-of-Flight Mass Spectrometry: Residential Coal Combustion. Environmental Science & Technology, 2018, 52, 2612-2617.	4.6	30
63	Formation of highly oxygenated organic molecules from aromatic compounds. Atmospheric Chemistry and Physics, 2018, 18, 1909-1921.	1.9	133
64	Insights into organic-aerosol sources via a novel laser-desorption/ionization mass spectrometry technique applied to one year of PM ₁₀ samples from nine sites in central Europe. Atmospheric Chemistry and Physics, 2018, 18, 2155-2174.	1.9	7
65	Large contribution of fossil fuel derived secondary organic carbon to water soluble organic aerosols in winter haze in China. Atmospheric Chemistry and Physics, 2018, 18, 4005-4017.	1.9	49
66	Influence of temperature on the molecular composition of ions and charged clusters during pure biogenic nucleation. Atmospheric Chemistry and Physics, 2018, 18, 65-79.	1.9	56
67	High contributions of vehicular emissions to ammonia in three European cities derived from mobile measurements. Atmospheric Environment, 2018, 175, 210-220.	1.9	42
68	Particle-bound reactive oxygen species (PB-ROS) emissions and formation pathways in residential wood smoke under different combustion and aging conditions. Atmospheric Chemistry and Physics, 2018, 18, 6985-7000.	1.9	31
69	Identification of secondary aerosol precursors emitted by an aircraft turbofan. Atmospheric Chemistry and Physics, 2018, 18, 7379-7391.	1.9	14
70	Production of particulate brown carbon during atmospheric aging of residential wood-burning emissions. Atmospheric Chemistry and Physics, 2018, 18, 17843-17861.	1.9	77
71	Advanced source apportionment of carbonaceous aerosols by coupling offline AMS and radiocarbon size-segregated measurements over a nearly 2-year period. Atmospheric Chemistry and Physics, 2018, 18, 6187-6206.	1.9	54
72	Source-Specific Health Risk Analysis on Particulate Trace Elements: Coal Combustion and Traffic Emission As Major Contributors in Wintertime Beijing. Environmental Science & Technology, 2018, 52, 10967-10974.	4.6	125

#	Article	IF	CITATIONS
73	Influence of the vapor wall loss on the degradation rate constants in chamber experiments of levoglucosan and other biomass burning markers. Atmospheric Chemistry and Physics, 2018, 18, 10915-10930.	1.9	19
74	Brown and Black Carbon Emitted by a Marine Engine Operated on Heavy Fuel Oil and Distillate Fuels: Optical Properties, Size Distributions, and Emission Factors. Journal of Geophysical Research D: Atmospheres, 2018, 123, 6175-6195.	1.2	62
75	Improved source apportionment of organic aerosols in complex urban air pollution using the multilinear engine (ME-2). Atmospheric Measurement Techniques, 2018, 11, 1049-1060.	1.2	28
76	Evolution of the chemical fingerprint of biomass burning organic aerosol during aging. Atmospheric Chemistry and Physics, 2018, 18, 7607-7624.	1.9	67
77	Contributions of residential coal combustion to the air quality in Beijing–Tianjin–Hebei (BTH), China: a case study. Atmospheric Chemistry and Physics, 2018, 18, 10675-10691.	1.9	60
78	Gas-phase composition and secondary organic aerosol formation from standard and particle filter-retrofitted gasoline direct injection vehicles investigated in a batch and flow reactor. Atmospheric Chemistry and Physics, 2018, 18, 9929-9954.	1.9	57
79	Source Apportionment of Brown Carbon Absorption by Coupling Ultraviolet–Visible Spectroscopy with Aerosol Mass Spectrometry. Environmental Science and Technology Letters, 2018, 5, 302-308.	3.9	60
80	Rapid growth of organic aerosol nanoparticles over a wide tropospheric temperature range. Proceedings of the National Academy of Sciences of the United States of America, 2018, 115, 9122-9127.	3.3	118
81	Sources of PM2.5 at an urban-industrial Mediterranean city, Marseille (France): Application of the ME-2 solver to inorganic and organic markers. Atmospheric Research, 2018, 214, 263-274.	1.8	29
82	Development, characterization and first deployment of an improved online reactive oxygen species analyzer. Atmospheric Measurement Techniques, 2018, 11, 65-80.	1.2	25
83	Source Apportionment of Inorganic Aerosols in Europe and Role of Biogenic VOC Emissions. Springer Proceedings in Complexity, 2018, , 375-379.	0.2	0
84	Wood combustion particles induce adverse effects to normal and diseased airway epithelia. Environmental Sciences: Processes and Impacts, 2017, 19, 538-548.	1.7	14
85	Contribution of bacteria-like particles to PM2.5 aerosol in urban and rural environments. Atmospheric Environment, 2017, 160, 97-106.	1.9	15
86	Characterization of Gas-Phase Organics Using Proton Transfer Reaction Time-of-Flight Mass Spectrometry: Aircraft Turbine Engines. Environmental Science & Technology, 2017, 51, 3621-3629.	4.6	6
87	Chemical composition, sources and secondary processes of aerosols in Baoji city of northwest China. Atmospheric Environment, 2017, 158, 128-137.	1.9	60
88	Review of Urban Secondary Organic Aerosol Formation from Gasoline and Diesel Motor Vehicle Emissions. Environmental Science & Technology, 2017, 51, 1074-1093.	4.6	348
89	Real-Time Characterization of Aerosol Particle Composition During Winter High-Pollution Events in China. , 2017, , 221-244.		0
90	Primary emissions and secondary aerosol production potential from woodstoves for residential heating: Influence of the stove technology and combustion efficiency. Atmospheric Environment, 2017, 169, 65-79.	1.9	48

#	Article	IF	CITATIONS
91	Gasoline cars produce more carbonaceous particulate matter than modern filter-equipped diesel cars. Scientific Reports, 2017, 7, 4926.	1.6	133
92	Long-term chemical analysis and organic aerosol source apportionment at nine sites in central Europe: source identification and uncertainty assessment. Atmospheric Chemistry and Physics, 2017, 17, 13265-13282.	1.9	78
93	Characterization of gas-phase organics using proton transfer reaction time-of-flight mass spectrometry: fresh and aged residential wood combustion emissions. Atmospheric Chemistry and Physics, 2017, 17, 705-720.	1.9	79
94	Secondary inorganic aerosols in Europe: sources and the significant influence of biogenic VOC emissions, especially on ammonium nitrate. Atmospheric Chemistry and Physics, 2017, 17, 7757-7773.	1.9	26
95	Argon offline-AMS source apportionment of organic aerosol over yearly cycles for an urban, rural, and marine site in northern Europe. Atmospheric Chemistry and Physics, 2017, 17, 117-141.	1.9	59
96	Impacts of meteorological uncertainties on the haze formation in Beijing–Tianjin–Hebei (BTH) during wintertime: a case study. Atmospheric Chemistry and Physics, 2017, 17, 14579-14591.	1.9	56
97	Evaluation of the absorption Ãngström exponents for traffic and wood burning in the Aethalometer-based source apportionment using radiocarbon measurements of ambient aerosol. Atmospheric Chemistry and Physics, 2017, 17, 4229-4249.	1.9	272
98	Assessing the influence of NO _{<i>x</i>} concentrations and relative humidity on secondary organic aerosol yields from <i>î±</i> -pinene photo-oxidation through smog chamber experiments and modelling calculations. Atmospheric	1.9	37
99	Chemistry and Physics, 2017, 17, 5035-5061. Modelling winter organic aerosol at the European scale with CAMx: evaluation and source apportionment with a VBS parameterization based on novel wood burning smog chamber experiments. Atmospheric Chemistry and Physics, 2017, 17, 7653-7669.	1.9	58
100	Organic aerosol source apportionment by offline-AMS over a full year in Marseille. Atmospheric Chemistry and Physics, 2017, 17, 8247-8268.	1.9	75
101	Constraining a hybrid volatility basis-set model for aging of wood-burning emissions using smog chamber experiments: a box-model study based on the VBS scheme of the CAMx model (v5.40). Geoscientific Model Development, 2017, 10, 2303-2320.	1.3	28
102	Characterization and source apportionment of organic aerosol using offline aerosol mass spectrometry. Atmospheric Measurement Techniques, 2016, 9, 23-39.	1.2	110
103	Labile Peroxides in Secondary Organic Aerosol. CheM, 2016, 1, 603-616.	5.8	132
104	Indoor terpene emissions from cooking with herbs and pepper and their secondary organic aerosol production potential. Scientific Reports, 2016, 6, 36623.	1.6	51
105	Contribution of methane to aerosol carbon mass. Atmospheric Environment, 2016, 141, 41-47.	1.9	12
106	Inorganic Salt Interference on CO ₂ ⁺ in Aerodyne AMS and ACSM Organic Aerosol Composition Studies. Environmental Science & Technology, 2016, 50, 10494-10503.	4.6	88
107	Identification of significant precursor gases of secondary organic aerosols from residential wood combustion. Scientific Reports, 2016, 6, 27881.	1.6	141
108	Urban increments of gaseous and aerosol pollutants and their sources using mobile aerosol mass spectrometry measurements. Atmospheric Chemistry and Physics, 2016, 16, 7117-7134.	1.9	31

#	Article	IF	CITATIONS
109	Aqueous phase oxidation of sulphur dioxide by ozone in cloud droplets. Atmospheric Chemistry and Physics, 2016, 16, 1693-1712.	1.9	47
110	New insights into PM _{2.5} chemical composition and sources in two major cities in China during extreme haze events using aerosol mass spectrometry. Atmospheric Chemistry and Physics, 2016, 16, 3207-3225.	1.9	300
111	Observation of viscosity transition in <i>α</i> -pinene secondary organic aerosol. Atmospheric Chemistry and Physics, 2016, 16, 4423-4438.	1.9	55
112	Fossil and non-fossil source contributions to atmospheric carbonaceous aerosols during extreme spring grassland fires in Eastern Europe. Atmospheric Chemistry and Physics, 2016, 16, 5513-5529.	1.9	35
113	Characterization of Gas-Phase Organics Using Proton Transfer Reaction Time-of-Flight Mass Spectrometry: Cooking Emissions. Environmental Science & Technology, 2016, 50, 1243-1250.	4.6	97
114	Size-Resolved Identification, Characterization, and Quantification of Primary Biological Organic Aerosol at a European Rural Site. Environmental Science & Technology, 2016, 50, 3425-3434.	4.6	57
115	Marine and urban influences on summertime PM2.5 aerosol in the Po basin using mobile measurements. Atmospheric Environment, 2015, 120, 447-454.	1.9	9
116	In situ, satellite measurement and model evidence on the dominant regional contribution to fine particulate matter levels in the Paris megacity. Atmospheric Chemistry and Physics, 2015, 15, 9577-9591.	1.9	92
117	Fossil vs. non-fossil sources of fine carbonaceous aerosols in four Chinese cities during the extreme winter haze episode of 2013. Atmospheric Chemistry and Physics, 2015, 15, 1299-1312.	1.9	163
118	Characterization of primary and secondary wood combustion products generated under different burner loads. Atmospheric Chemistry and Physics, 2015, 15, 2825-2841.	1.9	99
119	Inter-comparison of laboratory smog chamber and flow reactor systems on organic aerosol yield and composition. Atmospheric Measurement Techniques, 2015, 8, 2315-2332.	1.2	110
120	A new methodology to assess the performance and uncertainty of source apportionment models II: The results of two European intercomparison exercises. Atmospheric Environment, 2015, 123, 240-250.	1.9	63
121	Primary emissions and secondary organic aerosol formation from the exhaust of a flex-fuel (ethanol) vehicle. Atmospheric Environment, 2015, 117, 200-211.	1.9	59
122	Effects of alkylate fuel on exhaust emissions and secondary aerosol formation of a 2-stroke and a 4-stroke scooter. Atmospheric Environment, 2014, 94, 307-315.	1.9	24
123	Two-stroke scooters are a dominant source of air pollution in many cities. Nature Communications, 2014, 5, 3749.	5.8	126
124	High secondary aerosol contribution to particulate pollution during haze events in China. Nature, 2014, 514, 218-222.	13.7	3,582
125	Diurnal cycle of fossil and nonfossil carbon using radiocarbon analyses during CalNex. Journal of Geophysical Research D: Atmospheres, 2014, 119, 6818-6835.	1.2	82
126	Characterization of organic tracer compounds in PM2.5 at a semi-urban site in Beirut, Lebanon. Atmospheric Research, 2014, 143, 85-94.	1.8	15

#	Article	IF	CITATIONS
127	Radiocarbon analysis of elemental and organic carbon in Switzerland during winter-smog episodes from 2008 to 2012 – Part 1: Source apportionment and spatial variability. Atmospheric Chemistry and Physics, 2014, 14, 13551-13570.	1.9	89
128	Functional group composition of organic aerosol from combustion emissions and secondary processes at two contrasted urban environments. Atmospheric Environment, 2013, 75, 308-320.	1.9	16
129	Composition and Source Apportionment of Organic Aerosol in Beirut, Lebanon, During Winter 2012. Aerosol Science and Technology, 2013, 47, 1258-1266.	1.5	23
130	Towards a better understanding of the origins, chemical composition and aging of oxygenated organic aerosols: case study of a Mediterranean industrialized environment, Marseille. Atmospheric Chemistry and Physics, 2013, 13, 7875-7894.	1.9	87
131	Primary and secondary organic aerosol origin by combined gas-particle phase source apportionment. Atmospheric Chemistry and Physics, 2013, 13, 8411-8426.	1.9	96
132	Secondary organic aerosol formation from gasoline vehicle emissions in a new mobile environmental reaction chamber. Atmospheric Chemistry and Physics, 2013, 13, 9141-9158.	1.9	207
133	Identification of marine and continental aerosol sources in Paris using high resolution aerosol mass spectrometry. Journal of Geophysical Research D: Atmospheres, 2013, 118, 1950-1963.	1.2	142
134	Quantification of levoglucosan and its isomers by High Performance Liquid Chromatography – Electrospray Ionization tandem Mass Spectrometry and its applications to atmospheric and soil samples. Atmospheric Measurement Techniques, 2012, 5, 141-148.	1.2	53
135	Oligomer and SOA formation through aqueous phase photooxidation of methacrolein and methyl vinyl ketone. Atmospheric Environment, 2012, 49, 123-129.	1.9	64
136	Oxidation of Atmospheric Humic Like Substances by Ozone: A Kinetic and Structural Analysis Approach. Environmental Science & Technology, 2011, 45, 5238-5244.	4.6	47
137	Insights into the secondary fraction of the organic aerosol in a Mediterranean urban area: Marseille. Atmospheric Chemistry and Physics, 2011, 11, 2059-2079.	1.9	90
138	Primary sources of PM _{2.5} organic aerosol in an industrial Mediterranean city, Marseille. Atmospheric Chemistry and Physics, 2011, 11, 2039-2058.	1.9	95
139	Inter-comparison of source apportionment models for the estimation of wood burning aerosols during wintertime in an Alpine city (Grenoble, France). Atmospheric Chemistry and Physics, 2010, 10, 5295-5314.	1.9	261
140	Functional group composition of ambient and source organic aerosols determined by tandem mass spectrometry. Atmospheric Chemistry and Physics, 2010, 10, 7041-7055.	1.9	24
141	Comprehensive primary particulate organic characterization of vehicular exhaust emissions in France. Atmospheric Environment, 2009, 43, 6190-6198.	1.9	150
142	In-cloud processes of methacrolein under simulated conditions – Part 2: Formation of secondary organic aerosol. Atmospheric Chemistry and Physics, 2009, 9, 5107-5117.	1.9	69
143	In-cloud processes of methacrolein under simulated conditions – Part 3: Hygroscopic and volatility properties of the formed secondary organic aerosol. Atmospheric Chemistry and Physics, 2009, 9, 5119-5130.	1.9	26
144	Precursor ion scanning–mass spectrometry for the determination of nitro functional groups in atmospheric particulate organic matter. Analytica Chimica Acta, 2008, 618, 184-195.	2.6	24